ARTICLE
PUBLISHED ONLINE: 12 JANUARY 2014 | DOI: 10.1038/NCHEMBIO.1430
nature chemical biology

An optogenetic gene expression system with rapid activation and deactivation kinetics

Laura B Motta-Mena[1,2], Anna Reade[3,4], Michael J Mallory[5], Spencer Glantz[6], Orion D Weiner[3,4], Kristen W Lynch[5] & Kevin H Gardner[1,2,7]*

Optogenetic gene expression systems can control transcription with spatial and temporal detail unequaled with traditional inducible promoter systems. However, current eukaryotic light-gated transcription systems are limited by toxicity, dynamic range or slow activation and deactivation. Here we present an optogenetic gene expression system that addresses these shortcomings and demonstrate its broad utility. Our approach uses an engineered version of EL222, a bacterial light-oxygen-voltage protein that binds DNA when illuminated with blue light. The system has a large (>100-fold) dynamic range of protein expression, rapid activation (<10 s) and deactivation kinetics (<50 s) and a highly linear response to light. With this system, we achieve light-gated transcription in several mammalian cell lines and intact zebrafish embryos with minimal basal gene activation and toxicity. Our approach provides a powerful new tool for optogenetic control of gene expression in space and time.

Essential for many applications in biomedical research, inducible promoter systems enable the artificial control of gene transcription in eukaryotic cells[1,2]. Although many of these tools are widely useful, their reliance on small-molecule inducers (for example, doxycycline) limits their utility when precisely timed or localized induction is desired. Once applied, chemical inducers are also limited by their rate of diffusion (slowing activation), difficult removal (slowing deactivation) and potential off-target effects on normal cellular function. In contrast, light is a rapid and nontoxic stimulus that naturally regulates many different cellular processes in diverse settings[3]. To take advantage of these favorable properties, a variety of natural photosensitive proteins have recently been engineered into light-controlled transcriptional activators[4–11], providing the potential to regulate gene expression with previously unattainable spatiotemporal control. Nevertheless, these systems have major drawbacks that limit their use in a wide range of experiments. These disadvantages include toxicity[12], low transcriptional activation (<20-fold enhancement upon dark to light stimulation)[4–8,11], long deactivation times (>2 h)[10], use of exotic chromophores not found in vertebrates[4,5], potential interference of the active photoreceptor with endogenous signaling pathways[8] and the need for multiple protein components[4,6,7,9,11].

To address these limitations, we developed a new inducible promoter system using the EL222 bacterial transcription factor[13], which only contains the minimal elements needed for light-dependent transcriptional activation: a photosensory LOV[14] domain and a helix-turn-helix (HTH) DNA-binding domain. In the dark, the LOV domain binds the HTH domain, covering the HTH 4α helix essential to dimerization and DNA binding[13]. Blue light illumination (450 nm) triggers the photochemical formation of a protein-flavin adduct within the LOV domain, disrupting inhibitory LOV-HTH interactions and allowing EL222 to dimerize and bind DNA[15,16]. These structural changes spontaneously reverse in the dark, rapidly inactivating EL222 (τ ~11 s at 37 °C (ref. 17)). Within the native *Erythrobacter litoralis* HTCC2594 host, we observed light-dependent activation of genes adjacent to genomic EL222-binding sites, implicating this protein as a photosensitive transcription factor[15].

Our mechanistic understanding of EL222 paves the way for its use in a single-protein component system for light-dependent gene activation. Here we report that a minimally engineered variant of EL222 activates transcription in different eukaryotic systems upon stimulation with moderate levels of blue light. With this method, we demonstrate over 200-fold upregulation of gene expression from an EL222-responsive luciferase reporter in 293T cells illuminated with levels of blue light compatible with robust cellular growth. In contrast, dark-state and red light controls show changes of less than twofold, establishing minimal leakiness under noninducing conditions. Our system has rapid activation (<10 s) and deactivation kinetics (<50 s), which compare favorably to the <2-h turn-off kinetics of a recently developed LOV-based transcriptional system[10]. Furthermore, our system can achieve functional regulation of cellular processes, as we demonstrate for light-gated regulation of splicing in T cells. Finally, we demonstrate that EL222 can be used for either global or tissue-specific light-dependent gene expression in zebrafish with minimal toxicity, expanding the repertoire of this expression system. Taken together, our data highlight the broad utility of the EL222 system and its strengths as an optogenetic tool.

RESULTS

Development of an inducible promoter system based on EL222

EL222, a small (222-residue) bacterial transcription factor, is the basis of our engineered expression system (**Fig. 1a**). Two N-terminal additions adapt this protein for eukaryotic applications: a VP16 transcriptional activation domain (AD)[18] and a nuclear localization signal (NLS) sequence (**Fig. 1a**). Immunoblot analysis confirmed that the resulting VP-EL222 fusion protein was expressed in 293T cells and distributed between the nucleus and cytoplasm (**Supplementary Results**, **Supplementary Fig. 1a**).

[1]Department of Biophysics, University of Texas Southwestern Medical Center, Dallas, Texas, USA. [2]Department of Biochemistry, University of Texas Southwestern Medical Center, Dallas, Texas, USA. [3]Cardiovascular Research Institute, University of California–San Francisco, San Francisco, California, USA. [4]Department of Biochemistry and Biophysics, University of California–San Francisco, San Francisco, California, USA. [5]Department of Biochemistry and Biophysics, University of Pennsylvania, Philadelphia, Pennsylvania, USA. [6]Department of Bioengineering, University of Pennsylvania, Philadelphia, Pennsylvania, USA. [7]Structural Biology Initiative, Advanced Science Research Center, City University of New York, New York, New York, USA. *e-mail: Kevin.Gardner@asrc.cuny.edu

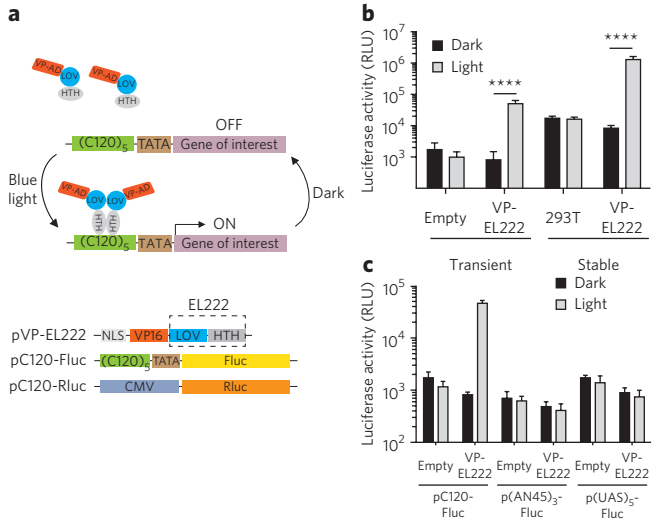

Figure 1 | Model for the EL222-based light-inducible gene expression system. (**a**) Top, the VP-EL222 protein consists of the transcriptional AD from the VP16 protein fused to EL222. In the dark, VP-EL222 is unable to bind DNA; however, exposure to blue light triggers a photochemical reaction between the LOV domain and its flavin chromophore, which activates the attached HTH domain to bind DNA and turn on gene transcription. Bottom, schematic representations of the DNA constructs used in this work. (**b**) For transient transfections, cells were transfected with either empty vector (containing only VP16 AD) or pVP-EL222 and pC120-Fluc plus an internal control plasmid pCMV-Rluc. For stable transfections, cells stably expressing VP-EL222 protein and wild-type 293T cells were transiently transfected with pC120-Fluc and pCMV-Rluc. Cells were kept in the dark or illuminated with blue light pulses (465 nm; 20 s on, 60 s off; 8 W m^{-2}) for 24 h (transient) or 12 h (stable) (n = 3 independent experiments, each performed in triplicate per condition). (**c**) Cells were transiently transfected with either empty vector or pVP-EL222 and one of three reporter constructs, pC120-Fluc, $p(AN45)_3$-Fluc or $p(UAS)_5$-Fluc, and kept in the dark or illuminated with blue light pulses (465 nm; 20 s on, 60 s off; 8 W m^{-2}) for 24 h. Levels of luciferase activity are shown (one experiment performed in triplicate per condition). ****$P < 0.0001$ using two-tailed Student's t-test. All data are represented as mean ± s.d.

To test the potency of the VP-EL222 transactivator system, we constructed a reporter vector containing the gene encoding firefly luciferase (Fluc) under the control of five copies of the EL222-binding clone 1–20 bp (C120)[15] sequence and a TATA box promoter (pC120-Fluc) (**Fig. 1a**). In transient transfections, 293T cells expressing VP-EL222 showed elevated luciferase with pulsed blue light illumination (24 h of 20 s on, 60 s off cycles; 8 W m^{-2} at 465 nm) compared to dark-state control cells (**Fig. 1b**). The light-driven upregulation of luciferase required EL222 as transfection of a vector containing only the VP16 AD (empty vector) showed effectively no activation of the pC120-Fluc reporter in any condition. Notably, the luciferase levels observed between cells expressing VP16 AD alone and the dark-state VP-EL222 cells are similar, establishing that VP-EL222 protein has minimal dark-state activity (as seen with *in vitro* DNA-binding assays[13,15]) and attributing background levels to basal activation of the reporter construct itself.

To quantify the transcriptional fold change of pC120-Fluc, we normalized the firefly luciferase values to an internal vector control (transfected with both pVP-EL222 and pC120-Fluc), which used the constitutive CMV promoter to drive expression of *Renilla* luciferase (Rluc). We calculated that cells transfected with VP-EL222 showed 216-fold upregulation of luciferase relative to cells transfected with empty vector when illuminated with blue light (**Supplementary Fig. 1b**). In contrast, cells kept in the dark showed only a twofold change, as expected from the low affinity of EL222 for DNA in the dark[13,15]. Taken together, these results demonstrate a net 108-fold increase in luciferase expression arising directly from illumination.

For maximum utility, specificity in inducible promoter systems is essential, both with target DNA sequences and with input stimuli, to avoid off-target effects. For the former, we previously investigated the *in vitro* specificity of EL222 with variants of the C120 DNA, showing that changes in a single base pair reduce EL222's affinity for its cognate sites by over tenfold[15]. Here we show that VP-EL222 retains its selectivity for C120 DNA in 293T cells, as measured by the increased expression from the pC120-Fluc reporter compared to two control constructs (**Fig. 1c** and **Supplementary Fig. 1c**). The first control contains three copies of a lower affinity EL222 substrate called AN45 (ref. 13) ($p(AN45)_3$-Fluc), which binds EL222 approximately 30-fold more weakly than C120 (refs. 13,15). A second control contained five copies of the GAL4-binding upstream activation sequence (UAS) ($p(UAS)_5$-Fluc). In both cases, luciferase levels were low and invariant to illumination when transfected together with pVP-EL222. Critically, expression levels from the two control vectors are comparable to those from pC120-Fluc when VP-EL222 is present and kept in the dark. This demonstrates that the measured leakiness in our experiments arises from basal transcription from the minimal promoter and not spurious dark activation of VP-EL222 or by binding of any cellular factors to the C120 promoter. Lastly, we underscore that the minimal promoter and UAS sequences used here were obtained from commercial sources that have previously evaluated their background activity[19,20], establishing our system of VP-EL222 and pC120 as having comparable background as these widely used reagents.

Additional experiments confirmed that expression of pVP-EL222 in 293T cells did not substantially affect cell viability as compared to the pVP-empty control under both dark and light conditions (**Supplementary Fig. 2a**), suggesting that neither VP-EL222 itself, VP-EL222–driven transcription nor our illumination protocol generate any gross toxicity. Lastly, we found that VP-EL222 is not triggered by continuous red light, as luciferase levels from the pC120-Fluc reporter are comparable under dark and red light conditions (**Supplementary Fig. 2b,c**). This indicates that VP-EL222 is specifically activated by blue light, consistent with standard LOV photochemistry. Together these data demonstrate that the functional and photochemical properties inherent to EL222 are suitable for use in heterologous expression in mammalian cells.

Characterization of VP-EL222 in stably transfected cells

To reduce experimental variability caused by differential transfection efficiencies, we stably expressed VP-EL222 in 293T cells and transfected only the pC120-FLuc plasmid (**Fig. 1b** and **Supplementary Fig. 1b**). As a control, wild-type 293T cells (without VP-EL222) were also transfected with pC120-Fluc alone. Consistent with our pVP-EL222 transient transfection data, luciferase levels were greatly enhanced in stable VP-EL222 cells illuminated with blue light relative to cells left in the dark (162-fold dark-to-light enhancement after 12-h illumination with 20 s on, 60 s off cycle). Furthermore, we again observed that luciferase levels in VP-EL222–expressing cells kept in the dark were comparable to those measured from wild-type 293T cells in both conditions. These results establish that the VP-EL222 system can generate high reporter gene expression in both transient and stable transfection experiments and that dark-state leakiness stems from basal activation of the pC120-Fluc vector itself.

A key advantage of a light-switchable promoter system is the ease of tuning gene expression levels by modifying illumination

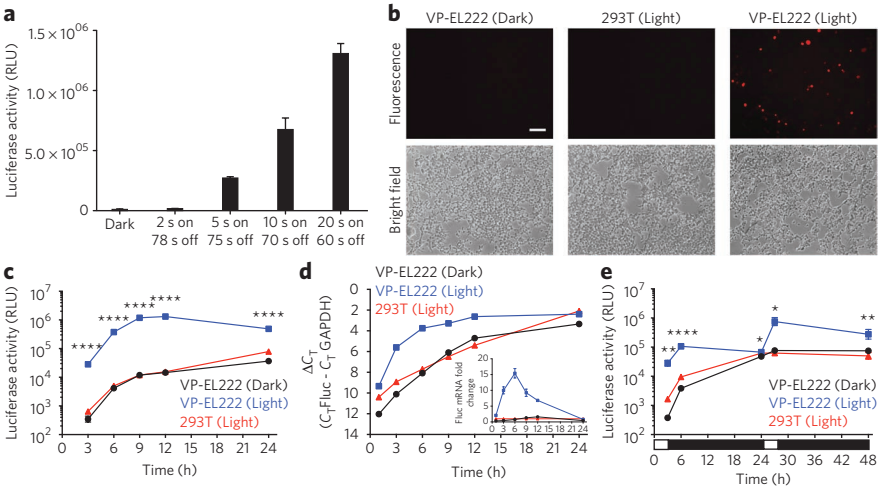

Figure 2 | Dose-dependent activation and photoreversibility of gene expression by VP-EL222. Cells stably expressing VP-EL222 protein (VP-EL222 cells) and wild-type 293T cells were transiently transfected with pC120-Fluc and illuminated with blue light pulses (20 s on, 60 s off) for 12 h, unless otherwise indicated. (**a**) Luciferase activity levels in VP-EL222 cells treated with blue light pulses of varying duration or kept in the dark. (**b**) Representative images of VP-EL222 and wild-type 293T cells transfected with pC120-mCherry and left in the dark or illuminated for 24 h. Scale bar, 100 μm. (**c**) Luciferase activity levels in wild-type 293T and VP-EL222 cells illuminated or kept in the dark for the indicated times. (**d**) Luciferase mRNA levels quantified by qPCR from wild-type 293T and VP-EL222 cells treated with blue light for the indicated times or kept in the dark. Normalized ΔC_T ($\Delta C_T = C_T$ Fluc $- C_T$ GAPDH) values are shown. Inset shows fold change in luciferase mRNA in VP-EL222 dark- and light-treated samples relative to the light-treated 293T control. (**e**) VP-EL222 and wild-type 293T cells were illuminated for two separate 3-h periods (white box), each separated by a 21-h dark period (black box). Controls were kept in the dark for the entire experiment. Luciferase activity levels were measured at the indicated time points. In all panels, one experiment was performed in triplicate per condition. $^*P < 0.05$; $^{**}P < 0.01$; $^{****}P < 0.0001$ using two-tailed Student's *t*-test. All data are represented as mean ± s.d.

protocols. We investigated the effects of modifying one such parameter, the duration of the on-off duty cycle, by examining luciferase expression off the pC120-Fluc reporter in the VP-EL222 stable cell line (**Fig. 2a**). Within a constant 80-s period, we observed an expected dose-dependent increase in luciferase with increasing duration of illumination during each cycle, with a linear correlation between luciferase levels and illumination times for periods of 5 s or greater. In addition to producing luciferase at levels easily quantified by enzymatic output, VP-EL222 is capable of expressing proteins at levels sufficient to be detected by western blotting (luciferase; **Supplementary Fig. 3**) or fluorescence microscopy (mCherry; **Fig. 2b**). In both cases, signals were detectable only in the presence of VP-EL222 and following blue light illumination.

Turning from steady-state measurements to the kinetics of gene expression, we examined protein and mRNA levels as a function of illumination time. To do so, we measured the luciferase activities of VP-EL222–expressing cells transfected with pC120-Fluc and incubated cells in the dark or illuminated them with a 20 s on, 60 s off protocol for the indicated times in **Figure 2c**. As a control, luciferase levels were also measured in wild-type 293T cells transfected with pC120-Fluc and illuminated with blue light pulses. We observed that luciferase activity was rapidly induced, with 80-fold increases observed over the VP-EL222 dark-state control after only 3 h. Induction levels further increased slightly to around 90-fold by 6 h and plateaued after 9 h at 100-fold. Notably, luciferase activity began to drop slightly between 12 h and 24 h; nevertheless, after 24 h, luciferase expression remained >20-fold above background expression. Although we detected a time-dependent increase in luciferase activity in VP-EL222 cells kept in the dark, this was virtually identical to 293T control values and significantly lower than from comparable illuminated VP-EL222 cells ($P < 0.0001$; **Fig. 2c**).

In parallel, we measured luciferase mRNA levels using qPCR (**Fig. 2d**), quantifying the relative expression level in each sample with a normalized cycle threshold value (ΔC_T) ($\Delta C_T = C_T$ Fluc $- C_T$ GAPDH). As expected, the ΔC_T values for light-treated VP-EL222 samples were smaller than those measured for dark-treated VP-EL222 and light-treated 293T samples. These ΔC_T values were used to calculate luciferase mRNA fold changes in VP-EL222 dark- and light-treated samples relative to the light-treated 293T control. These analyses showed that luciferase mRNA spiked after 3 h of illumination, reaching a maximum at 6 h (~16-fold increase over 293T control; **Fig. 2d**). After 9 h of illumination, luciferase mRNA levels decreased to ninefold over 293T control before falling to less than twofold at 24 h. We note that these trends in luciferase transcript levels precede the corresponding trend in protein levels (**Fig. 2d**). These data suggest a loss of VP-EL222 transcriptional activity during extended illumination that is potentially due to a moderate decrease in VP-EL222 protein levels (**Supplementary Fig. 3**).

This time-dependent decrease led us to ask whether VP-EL222 could be reactivated after an initial round of illumination followed by a dark recovery period to allow for synthesis of fresh transcription factor. To do so, we monitored luciferase activity in wild-type 293T and stable VP-EL222 cells (both transfected with pC120-Fluc) that were initially illuminated with blue light (20 s on, 60 s off) for 3 h, incubated in the dark for 21 h, then again illuminated for 3 h (**Fig. 2e**). After the initial activation, luciferase levels elevated approximately 75-fold over dark control VP-EL222 cells. Once the light was removed, the absolute amount of luciferase activity remained elevated in the illuminated cells; however, luciferase background levels slowly increased in the dark control VP-EL222 cells, dropping the dark-to-light fold induction to near-background levels over 21 h (<1.5-fold difference between dark and light). After this recovery period, cells were illuminated for 3 h with pulsing blue light, increasing luciferase levels back to 11-fold over VP-EL222 dark-state controls. Following another 21-h dark recovery period, luciferase induction decreased to around 3.7-fold. Critically, similar luciferase levels were seen in dark-treated control VP-EL222 cells and illuminated wild-type 293T cells throughout, as observed previously. Therefore, the data show that light-triggered activation of VP-EL222 can generate multiple rounds of gene expression, enabling new experiments using transient increases in protein level.

Modeling transcriptional kinetics of VP-EL222 in cells

Aspects of these applications, linear dose-response (**Fig. 2a**) and favorable kinetic properties (**Fig. 2e**), are enabled by the intrinsically fast activation and deactivation kinetics of EL222. *In vitro* measurements reveal LOV domains activate via microsecond-to-millisecond timescale events[21,22], whereas deactivation by adduct cleavage occurs over seconds to hours[17,23]. Comparable activation-deactivation measurements for VP-EL222–driven transcription

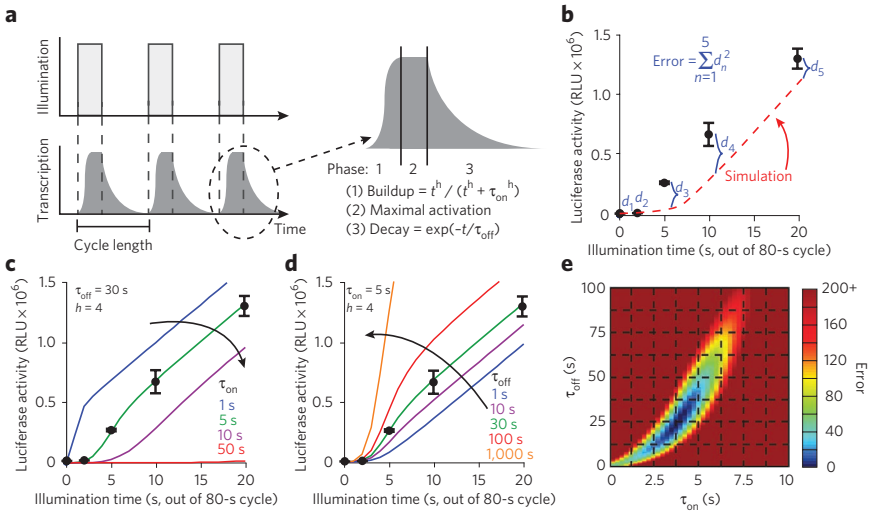

Figure 3 | Kinetic modeling of VP-EL222 activation. (**a**) Summary of the model used to describe VP-EL222 transcriptional activation, including three phases of transcriptional activity. Additional details are provided in Online Methods. (**b**) Data used for kinetic modeling (replotted showing mean ± s.d. from **Fig. 2a**) along with definition of least-squared error function. (**c**) Effect of varying τ_{on} on transcriptional activity. Given a τ_{off} of 30 s (estimated from *in vitro* measurements of EL222 deactivation[17]) and Hill coefficient of 4, average steady-state transcriptional activities at τ_{on} values between 1 s and 50 s were calculated using our model. The best agreement with experimental data was obtained with τ_{on} ~5 s. (**d**) Effect of varying τ_{off} on transcriptional activity. For a given τ_{on} of 5 s (based on **c**), average transcriptional activities at τ_{off} values between 1 s and 1,000 s were calculated. The best agreement with experimental error was obtained with τ_{off} ~30 s. (**e**) Grid search of τ_{on} and τ_{off} values (independently iterated for τ_{on} < 100s, τ_{off} < 100s), using the model, data and error function described above. The heat map indicates the value of error function; only the region with the error function < 200 (τ_{on} 1–10 s, τ_{off} = 1–100 s) is shown here.

within cells are complicated by slow reporter mRNA and protein turnover (for example, luciferase mRNA half-life is 3–5 h[24,25], and protein half-life is 3–4 h[26]), limiting the temporal resolution of many experiments that yield this information. As an alternative, we developed a kinetic model that correlates gene expression with the times required for VP-EL222 to initiate transcription upon illumination (τ_{on}) or cease in the dark (τ_{off}) (**Fig. 3a** and **Supplementary Notes 1** and **2**). This model lets us obtain information on second-timescale events from final end-point measurements of luciferase levels accumulated from repeatedly activating VP-EL222, each time gaining a burst of mRNA (**Fig. 2a**).

Coupled with an accompanying least-squared error analysis (**Fig. 3b**), this framework lets us determine how consistent different combinations of τ_{on} and τ_{off} values are with our experimental measurements. For activation, the observed lag in luciferase expression at short illumination times implies an initial τ_{on} delay of approximately several seconds for VP-EL222 to activate, bind DNA and initiate transcription. Our model exhibits an expected inverse relationship between gene expression and τ_{on}, with values near 5 s recapitulating our data most accurately (**Fig. 3c**). On deactivation, our model recapitulates a direct link between τ_{off} and luciferase levels, with optimal τ_{off} values of approximately 30 s (**Fig. 3d**). A more complete grid search of all values of τ_{on} and τ_{off} reveals a range of values compatible with our data (**Fig. 3e**). This range includes activation times of approximately 3–5 s, compatible with single-molecule measurements of transcriptional initiation rates[27] and the high level of VP-EL222 within 293T cells. The same analysis indicates τ_{off} values between 10–40 s; the shortest of these delays is consistent with our *in vitro* measurements of EL222 adduct cleavage (τ_{adduct} ~11 s at 37 °C[17]), suggesting that cellular factors have limited effects on this critical step. Taken together, these data suggest that VP-EL222 functions with rapid on-off kinetics in cells, a key advantage over other comparable systems[10].

Light-inducible expression of CELF2 protein in T cells

To test the utility of the VP-EL222 system in other cultured cell lines, we investigated its ability to drive the expression of a functionally active protein within the T cell–derived Jurkat splicing line 1 (JSL1) cell line[28]. The JSL1 cell line has been extensively used to study changes in alternative pre-mRNA splicing that occur in response to T-cell activation[28–30]. One protein implicated in such control is CUGBP and ETR-2 like factor 2 (CELF2)[31], an RNA-binding protein with a known role in splicing regulation in JSL1 cells and thymocytes following cellular stimulation[32]. Phorbol myristate acetate (PMA)-induced activation of JSL1 cells increases CELF2 expression, promoting its binding to regulatory sequences in target pre-mRNAs and affecting their processing[32]. Indeed, at high levels, CELF2 represses the inclusion of exon 6 in its own pre-mRNA[29,32,33], providing an assay to ascertain whether the VP-EL222 system could drive CELF2 overexpression sufficiently to confer light-dependent control of pre-mRNA splicing.

To examine this, we created a JSL1 cell line stably integrated with both the pVP-EL222 activator and a Flag-tagged CELF2 under the control of the EL222-specific C120 promoter (VP-EL222/CELF2 cells). VP-EL222/CELF2 cells incubated in the dark showed nearly no expression of Flag-CELF2 protein by immunoblot analysis (**Fig. 4a** and **Supplementary Fig. 4a**), whereas cells exposed to blue light for 24 h (20 s on, 60 s off) showed moderate Flag-CELF2 expression, indicating functional light-triggered activation of VP-EL222 in JSL1 cells. Notably, the levels of VP-EL222 protein itself decreased markedly (>50%) with light exposure (**Fig. 4a**), a more substantial decrease than that observed with 293T cells (**Fig. 2b**). Nevertheless, the small amount of VP-EL222 is sufficient to produce amounts of CELF2 protein readily detectable by western blotting.

To address the functional importance of light-induced Flag-CELF2 upregulation, we analyzed the splicing pattern of exon 6 of the endogenous CELF2 transcript by RT-PCR analysis using primers that specifically recognize the endogenous transcript and not the transfected cDNA. We found that blue light induced a moderate but statistically significant increase in the skipping of the CELF2 exon 6 in VP-EL222/CELF2 cells (P <0.05; **Fig. 4b** and **Supplementary Fig. 4b**), demonstrating light-regulated alternative splicing. Notably, blue light treatment had no discernible effects on exon 6 inclusion in wild-type JSL1 cells, underscoring the necessity of the photosensitive VP-EL222 in this process. Previous studies determined that PMA stimulation of JSL1 cells leads to a twofold increase in CELF2 protein[32], changing percent exon inclusion values by 20–30%[29]. In our experiment, light increases the amount of Flag-CELF2 protein fivefold over dark control; however, this does not detectably increase total CELF2, as seen by western blotting. This observation is consistent with known autoregulatory mechanisms that maintain stable CELF2 expression[32]. In addition, the fact that induction of Flag-CELF2 only marginally increases overall CELF2 protein is consistent with the relative effect we observed in CELF2 exon 6 skipping (20% to 25%).

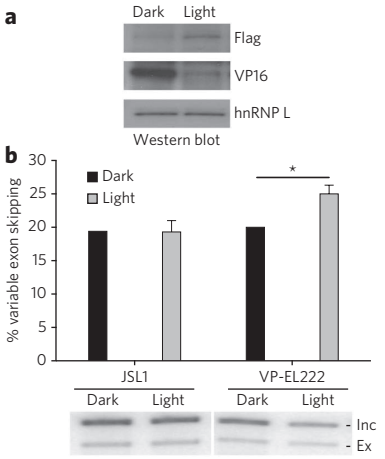

Figure 4 | Light-regulated gene expression of the splicing factor CELF2 using VP-EL222 in the T cell–derived JSL1 cell line. (**a**) Western blot analysis of protein lysates derived from JSL1 cells stably expressing both VP-EL222 and pC120-Flag-CELF2 (JSL1 VP-EL222/CELF2 cells) were illuminated for 24 h with either pulsing blue light (20 s on, 60 s off) or kept in the dark. An hnRNP L antibody was used as a loading control. (**b**) Percentage skipping of exon 6 in endogenous CELF2 gene for wild-type and VP-EL222/CELF2 JSL1 cells (VP-EL222) that were illuminated with pulsing blue light (20 s on, 60 s off) for 24 h or kept in the dark. The calculated exon skipping in illuminated samples was normalized relative to that measured in dark samples for each cell line. Below, representative RT-PCR gel showing the increase in exon skipping relative to inclusion. Inc, inclusion of exon; Ex, exclusion of exon. ($n = 2$ independent experiments, each performed with one replicate per condition). $^*P < 0.05$ using two-tailed Student's t-test. Data are represented as mean ± s.d.

VP-EL222 serves as a transcriptional activator *in vivo*

Transitioning from cell culture to intact multicellular organisms, we examined the capability of VP-EL222 to drive light-triggered gene expression in the zebrafish (*Danio rerio*). To do so, we microinjected the pC120-mCherry plasmid into zebrafish embryos at the one-cell stage, with or without 50 pg VP-EL222 mRNA (**Fig. 5a**). When embryos microinjected with VP-EL222 mRNA and pC120-mCherry were illuminated with constant blue light (14 mW m^{-2}), mCherry fluorescence was readily detected after only 5 h (70% epiboly stage). After 22 h of illumination (24 h post fertilization (h.p.f.) stage), 100% of the 50 embryos analyzed had marked mCherry fluorescence, the level of which was nicely illustrated by a *Z*-stack series of an embryo at 70% epiboly with VP-EL222–driven mCherry expression (**Supplementary Video 1**). In contrast, when VP-EL222/pC120-mCherry embryos were left in the dark or did not receive VP-EL222 mRNA, no fluorescence was detected (0/50 embryos in each set; **Supplementary Video 2**). These results show that VP-EL222 can rapidly and robustly activate transcription in developing zebrafish in a light-dependent manner.

Complementing these embryo-wide expression studies, we examined the ability to use VP-EL222 for light-inducible, tissue-specific gene expression. For this, we constructed a dual-promoter plasmid encoding the VP-EL222 ORF controlled by the zebrafish cardiac *myl7* (myosin light polypeptide 7) promoter[34] and the mCherry ORF controlled by the EL222-specific C120 promoter. Zebrafish embryos microinjected with p*myl7*-VP-EL222/C120-mCherry plasmid and illuminated with constant blue light, but not dark counterparts, showed noticeable mCherry fluorescence that was specifically localized in the developing heart (**Fig. 5b** and **Supplementary Video 3**).

Finally, we examined the toxicity of VP-EL222 in zebrafish embryos, comparing groups that were illuminated after being titrated with different amounts of VP-EL222 or GFP mRNA (**Supplementary Fig. 5**). We found that a small amount of VP-EL222 (50 pg mRNA) was sufficient to elicit high levels of mCherry expression (**Fig. 5a**) with only minimal morphological effects (81% unaffected embryos for VP-EL222 versus 93% for GFP) or toxicity (<10% severely affected or dead) relative to comparable GFP controls. Increasing amounts of microinjected VP-EL222 mRNA up to 150 pg affected more embryos, but these effects (~60% embryos unaffected; severely affected plus dead embryos made up less than 25%) remained constant above this level. These results suggest that VP-EL222 protein is only moderately toxic to zebrafish, much less so than that observed for a cryptochrome-based light-driven transcription system[12].

DISCUSSION

Here we describe a new inducible gene expression system that confers high-level, blue light–sensitive control of transcriptional initiation to human cell lines and zebrafish embryos. Using the naturally occurring EL222 transcription factor[13,15–17], we take advantage of LOV domain photochemistry and subsequent conformational changes, as seen in other LOV domains and the related Per-ARNT-Sim sensors[35,36].

More broadly, this system has several benefits compared with alternative photocontrolled gene expression methods. First, VP-EL222 functions in a range of eukaryotic cell settings, enabled by the use of widely available flavin chromophores and thus eliminating the need to supply exogenous cofactors or precursors[4,5]. Additionally, VP-EL222 has low toxicity (**Supplementary Fig. 2a**) and basal transcriptional activity in cell lines and zebrafish (**Figs. 1** and **5**); both features may be related to the absence of intact C120 targets in the human and zebrafish genomes (**Supplementary Table 1**). Second, the required VP-EL222 photochemistry is triggered with low-intensity blue light (8 W m^{-2} = 0.008 mW mm^{-2}), less intense than that required to activate channel rhodopsin–driven optogenetic applications (for example, 5 mW mm^{-2})[37]. Third, VP-EL222 uses only a single 33-kDa protein with a directly

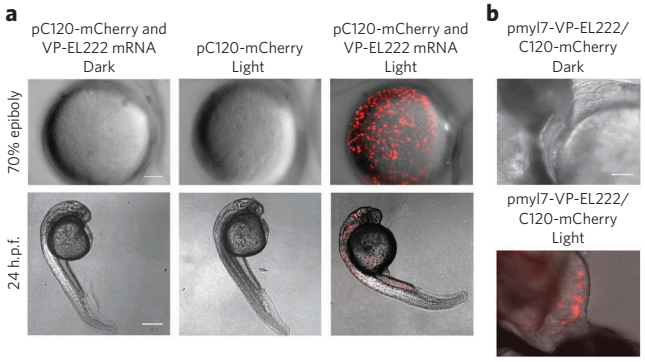

Figure 5 | VP-EL222 robustly activates reporter gene expression in the developing zebrafish embryo in a light-dependent manner. (**a**) Representative images of zebrafish embryos after injection with both VP-EL222 mRNA and pC120-mCherry DNA or pC120-mCherry DNA alone. The embryos were kept in the dark or illuminated with constant blue light for 5 h (70% epiboly stage) or 22 h (24 h.p.f. stage) beginning at 2 h.p.f. ($n = 50$ embryos per condition). Each image is a maximum intensity projection of a fluorescent *Z*-stack merged with its corresponding bright field image. Top scale bar, 100 μm; bottom scale bar, 300 μm. (**b**) Visualization of mCherry fluorescence in the zebrafish heart in illuminated (as described above) versus control embryos after injection with a dual promoter vector that contains VP-EL222 and mCherry under the control of the cardiomyocyte-specific *myl7* promoter and the EL222-specific C120 promoter; respectively. mCherry and bright field channels were merged. Scale bar, 50 μm.

regulated DNA-binding step, simplifying genetic manipulation and tuning compared to light-dependent two-hybrid systems[4,6,7,9,11] or those that must tie into existing cellular signaling pathways[8]. Finally, VP-EL222 quickly activates and resets after illumination (**Fig. 3e**), facilitating transient-expression experiments and predictable dose-response behavior.

A final characteristic of VP-EL222 that warrants explicit discussion is the background expression under noninducing conditions. This can arise from two sources: (i) residual dark-state binding of EL222 to C120 sites and (ii) spurious activation of the minimal promoter from the reporter vector itself. We consistently observed that pC120-Fluc alone produced similar activation levels as dark-state VP-EL222–expressing cells transfected with pC120-Fluc (**Figs. 1** and **2**), strongly suggesting that any basal activation comes primarily from pC120-Fluc itself. Notably, these background expression levels are equivalent to those from a commercial GAL4-driven expression vector (**Fig. 1c**) containing widely used consensus UAS sites[19]. From a practical standpoint, it is also clear that any background expression we observed with VP-EL222 had minimal effects among many different types of experiments (**Figs. 2b** and **5a** and **Supplementary Fig. 3**). We appreciate that some other applications may be affected by this low background activation (for example, overexpression of certain enzymes); therefore, we present raw activity and abundance values in formats that most clearly demonstrate background expression levels (**Figs. 1** and **2**) to inform users of these methods of potential contributions that may arise from this source. Finally, we also note that promoter modifications may establish lower background expression, as demonstrated in the optimization of Tet-responsive systems[38].

Recently, a variety of light-inducible systems for regulating gene expression in mammalian cells[8,10] have been reported. Such systems fall roughly in two categories, based on their regulation of (i) DNA binding or (ii) recruitment of a transcriptional AD to a DNA-bound protein. The first group is typified by a highly modified version of the Vivid LOV protein, which can strongly activate gene transcription (>200-fold)[10], albeit with somewhat nonideal dose-response behavior and deactivation kinetics owing to a long-lived photoadduct (half-life = 2 h). The second strategy is more widely used, with a flexible two-hybrid type implementation involving TALE DNA-binding domains with a light-inducible CRY2-CIB interaction to reversibly recruit a transcriptional AD[39]. Although this system can be customized to target many DNA sites, it also uses TALE domains constitutively bound to DNAs, potentially altering endogenous protein-DNA interactions nearby. In contrast, the direct photocontrol of VP-EL222 DNA binding minimizes the chance for alterations in the dark**.** Although VP-EL222 is currently restricted to one binding site, prior HTH engineering studies[40] suggest that this could be changed in VP-EL222 variants.

Looking ahead, we envision many cell and synthetic biology applications with different requirements for features of light-driven transcriptional regulators, such as maximal kinetic resolution or sensitivity. Mechanism-based approaches, such as EL222 variants engineered with shorter- and longer-lived photoactive states[17], will be essential to developing reagents optimized for each of these applications. Such engineering is facilitated by correlations between *in vitro* and cellular properties (for example, deactivation times), enabling rapid and simple screening of mutants. Coupled with the ability to control epigenetic or other cellular machinery to specific DNA sites in a light-dependent manner with other VP-EL222 variants, we anticipate that this protein will enable an even wider range of applications in the future.

Received 20 June 2013; accepted 19 November 2013;
published online 12 January 2014

METHODS

Methods and any associated references are available in the online version of the paper.

References

1. Weber, W. & Fussenegger, M. Inducible product gene expression technology tailored to bioprocess engineering. *Curr. Opin. Biotechnol.* **18**, 399–410 (2007).
2. Weber, W. & Fussenegger, M. Emerging biomedical applications of synthetic biology. *Nat. Rev. Genet.* **13**, 21–35 (2012).
3. Briggs, W.R. & Spudich, J.L. *Handbook of Photosensory Receptors* (Wiley-VCH, 2005).
4. Shimizu-Sato, S., Huq, E., Tepperman, J.M. & Quail, P.H. A light-switchable gene promoter system. *Nat. Biotechnol.* **20**, 1041–1044 (2002).
5. Levskaya, A. *et al.* Synthetic biology: engineering *Escherichia coli* to see light. *Nature* **438**, 441–442 (2005).
6. Yazawa, M., Sadaghiani, A.M., Hsueh, B. & Dolmetsch, R.E. Induction of protein-protein interactions in live cells using light. *Nat. Biotechnol.* **27**, 941–945 (2009).
7. Kennedy, M.J. *et al.* Rapid blue-light-mediated induction of protein interactions in living cells. *Nat. Methods* **7**, 973–975 (2010).
8. Ye, H., Daoud-El Baba, M., Peng, R.W. & Fussenegger, M. A synthetic optogenetic transcription device enhances blood-glucose homeostasis in mice. *Science* **332**, 1565–1568 (2011).
9. Ohlendorf, R., Vidavski, R.R., Eldar, A., Moffat, K. & Moglich, A. From dusk till dawn: one-plasmid systems for light-regulated gene expression. *J. Mol. Biol.* **416**, 534–542 (2012).
10. Wang, X., Chen, X. & Yang, Y. Spatiotemporal control of gene expression by a light-switchable transgene system. *Nat. Methods* **9**, 266–269 (2012).
11. Polstein, L.R. & Gersbach, C.A. Light-inducible spatiotemporal control of gene activation by customizable zinc finger transcription factors. *J. Am. Chem. Soc.* **134**, 16480–16483 (2012).
12. Liu, H., Gomez, G., Lin, S., Lin, S. & Lin, C. Optogenetic control of transcription in zebrafish. *PLoS ONE* **7**, e50738 (2012).
13. Nash, A.I. *et al.* Structural basis of photosensitivity in a bacterial light-oxygen-voltage/helix-turn-helix (LOV-HTH) DNA-binding protein. *Proc. Natl. Acad. Sci. USA* **108**, 9449–9454 (2011).
14. Huala, E. *et al. Arabidopsis* NPH1—a protein kinase with a putative redox-sensing domain. *Science* **278**, 2120–2123 (1997).
15. Rivera-Cancel, G., Motta-Mena, L.B. & Gardner, K.H. Identification of natural and artificial DNA substrates for light-activated LOV-HTH transcription factor EL222. *Biochemistry* **51**, 10024–10034 (2012).
16. Zoltowski, B.D., Motta-Mena, L.B. & Gardner, K.H. Blue light–induced dimerization of a bacterial LOV-HTH DNA-binding protein. *Biochemistry* **52**, 6653–6661 (2013).
17. Zoltowski, B.D., Nash, A.I. & Gardner, K.H. Variations in protein-flavin hydrogen bonding in a light, oxygen, voltage domain produce non-Arrhenius kinetics of adduct decay. *Biochemistry* **50**, 8771–8779 (2011).
18. Sadowski, I., Ma, J., Triezenberg, S. & Ptashne, M. GAL4–VP16 is an unusually potent transcriptional activator. *Nature* **335**, 563–564 (1988).
19. Sadowski, I., Bell, B., Broad, P. & Hollis, M. GAL4 fusion vectors for expression in yeast or mammalian cells. *Gene* **118**, 137–141 (1992).
20. Swanson, B., Fan, F. & Wood, K. in *Promega Corporation* Vol. 17 3–5 (Cell Notes, 2007).
21. Chen, E., Swartz, T.E., Bogomolni, R.A. & Kliger, D.S.A. LOV story: the signaling state of the phot1 LOV2 photocycle involves chromophore-triggered protein structure relaxation, as probed by far-UV time-resolved optical rotatory dispersion spectroscopy. *Biochemistry* **46**, 4619–4624 (2007).
22. Kennis, J.T. *et al.* Primary reactions of the LOV2 domain of phototropin, a plant blue-light photoreceptor. *Biochemistry* **42**, 3385–3392 (2003).
23. Harper, S.M., Neil, L.C., Day, I.J., Hore, P.J. & Gardner, K.H. Conformational changes in a photosensory LOV domain monitored by time-resolved NMR spectroscopy. *J. Am. Chem. Soc.* **126**, 3390–3391 (2004).
24. Pan, Y.X., Chen, H. & Kilberg, M.S. Interaction of RNA-binding proteins HuR and AUF1 with the human ATF3 mRNA 3′-untranslated region regulates its amino acid limitation-induced stabilization. *J. Biol. Chem.* **280**, 34609–34616 (2005).
25. Qian, X. *et al.* Posttranscriptional regulation of IL-23 expression by IFN-γ through tristetraprolin. *J. Immunol.* **186**, 6454–6464 (2011).
26. Thompson, J.F., Hayes, L.S. & Lloyd, D.B. Modulation of firefly luciferase stability and impact on studies of gene regulation. *Gene* **103**, 171–177 (1991).
27. Larson, D.R., Zenklusen, D., Wu, B., Chao, J.A. & Singer, R.H. Real-time observation of transcription initiation and elongation on an endogenous yeast gene. *Science* **332**, 475–478 (2011).
28. Lynch, K.W. & Weiss, A. A model system for activation-induced alternative splicing of CD45 pre-mRNA in T cells implicates protein kinase C and Ras. *Mol. Cell. Biol.* **20**, 70–80 (2000).

29. Ip, J.Y. *et al.* Global analysis of alternative splicing during T-cell activation. *RNA* **13**, 563–572 (2007).
30. Martinez, N.M. *et al.* Alternative splicing networks regulated by signaling in human T cells. *RNA* **18**, 1029–1040 (2012).
31. Faustino, N.A. & Cooper, T.A. Identification of putative new splicing targets for ETR-3 using sequences identified by systematic evolution of ligands by exponential enrichment. *Mol. Cell. Biol.* **25**, 879–887 (2005).
32. Mallory, M.J. *et al.* Signal- and development-dependent alternative splicing of LEF1 in T cells is controlled by CELF2. *Mol. Cell. Biol.* **31**, 2184–2195 (2011).
33. Dembowski, J.A. & Grabowski, P.J. The CUGBP2 splicing factor regulates an ensemble of branchpoints from perimeter binding sites with implications for autoregulation. *PLoS Genet.* **5**, e1000595 (2009).
34. Yelon, D., Horne, S.A. & Stainier, D.Y. Restricted expression of cardiac myosin genes reveals regulated aspects of heart tube assembly in zebrafish. *Dev. Biol.* **214**, 23–37 (1999).
35. Harper, S.M., Neil, L.C. & Gardner, K.H. Structural basis of a phototropin light switch. *Science* **301**, 1541–1544 (2003).
36. Scheuermann, T.H. *et al.* Allosteric inhibition of hypoxia inducible factor-2 with small molecules. *Nat. Chem. Biol.* **9**, 271–276 (2013).
37. Mattis, J. *et al.* Principles for applying optogenetic tools derived from direct comparative analysis of microbial opsins. *Nat. Methods* **9**, 159–172 (2012).
38. Loew, R., Heinz, N., Hampf, M., Bujard, H. & Gossen, M. Improved Tet-responsive promoters with minimized background expression. *BMC Biotechnol.* **10**, 81 (2010).
39. Konermann, S. *et al.* Optical control of mammalian endogenous transcription and epigenetic states. *Nature* **500**, 472–476 (2013).
40. Krueger, M., Scholz, O., Wisshak, S. & Hillen, W. Engineered Tet repressors with recognition specificity for the tetO-4C5G operator variant. *Gene* **404**, 93–100 (2007).

Acknowledgments

This work was funded by grants from the US National Institutes of Health (R01 GM081875 and GM106239 to K.H.G.; R01 GM103383 to K.W.L.; R01 GM096164 to O.D.W.), Cancer Prevention and Research Institute of Texas (RP130312), Defense Advanced Research Projects Agency (Living Foundries HR0011-12-C-0068 to B. Chow (University of Pennsylvania), supporting S.G.) and the Robert A. Welch Foundation (I-1424 to K.H.G.). K.H.G. is the Virginia Lazenby O'Hara Chair in Biochemistry and W.W. Caruth Scholar in Biomedical Research. A.R. was supported by a National Science Foundation Graduate Research Fellowship. We thank S.L. McKnight and P.R. Potts (both at UT Southwestern Medical Center) for generously providing constructs.

Author contributions

L.B.M.-M., A.R., O.D.W., K.W.L. and K.H.G. conceived and designed the experiments. L.B.M.-M., A.R. and M.J.M. performed the experiments. L.B.M.-M., A.R., M.J.M., O.D.W., K.W.L. and K.H.G. analyzed the data, with S.G. and K.H.G. generating the kinetic model. L.B.M.-M. and K.H.G. wrote the paper.

Competing financial interests

The authors declare competing financial interests: details accompany the online version of the paper.

Additional information

Supplementary information is available in the online version of the paper. Reprints and permissions information is available online at http://www.nature.com/reprints/index.html. Correspondence and requests for materials should be addressed to K.H.G.

ONLINE METHODS

Vector construction. DNA containing residues 14–222 of EL222 (ref. 13) was cloned into the pVP16 (Clontech) vector to obtain pVP-EL222. The pVP-EL222-puro plasmid was created by PCR amplification of VP16-EL222 ORF and cloning into pIRESpuro (Clontech). Five tandem copies of the 20-bp clone-1 (C120) sequence[15] were chemically synthesized (GeneArt) and inserted into the pGL4.23(*luc2*/minP) (Promega) to make pGL4-C120-Fluc. pcDNA-C120-Fluc was created by PCR-amplifying the C120 sequence and the firefly luciferase ORF from the pGL4-C120-Fluc vector and cloning both into pcDNA3.1+ (Invitrogen). pGL4-C120-mCherry was created by PCR amplification of mCherry ORF and subcloning into pGL4-C120-Fluc to replace the luciferase ORF. The sequences and maps of the constructs used in this study are provided in **Supplementary Note 3**.

Cell culture, transfections, light induction and cell viability assay. 293T (ATCC) and JSL1 cells were cultured at 37 °C in 5% CO_2 in DMEM (Thermo Scientific) and RPMI (Gibco), respectively. Both did not contain phenol red and were supplemented with 5–10% FBS (Gibco) and 1% penicillin-streptomycin solution.

To make the 293T VP-EL222 stable cell line, cells were transfected with pVP-EL222-puro plasmid and allowed to recover for 3 d. Afterward, cells were serially diluted into medium containing 2 μg ml^{-1} of puromycin (Gibco) and grown for 1–2 weeks. Puromycin-resistant clones were expanded and analyzed for VP-EL222 expression by western blotting. To make a JSL1 VP-EL222 stable cell line, cells were diluted in medium containing 0.2 mg ml^{-1} zeocin (Gibco). The JSL1 VP-EL222/C120-Flag-CELF2 double stable cell line was made by transfecting the JSL1 VP-EL222 stable cell line with pC120-Flag-CELF2 plasmid. After transfection, cells were diluted in medium containing 0.6 mg ml^{-1} G418 sulfate (Gibco). Drug-resistant clones were screened by RT-PCR for genomic integration of the pC120-Flag-CELF2.

For transient transfections, 293T cells were plated at 2×10^5 cells per well in 24-well plates and transfected with 0.5 μg pGL4.23-C120-Fluc DNA the same day using lipofectamine (Invitrogen). pVP-EL222 or pVP-empty, pGL4-C120-Fluc and pGL4.75(hRluc/CMV) (Promega) constructs were transfected using a 5:1:0.04 ratio, respectively. Twenty-four hours after transfection, a blue LED panel (465 nm, 2501BU, LED Wholesalers) was placed above the plate. The intensity of the light received by cells was measured to be 39.7 mol s^{-1} m^{-2} (equivalent to 8 W m^{-2}) using the LI-190 Quantum Sensor and LI-250A light meter (LI-COR Biosciences). The LED panel was connected to an electronic intervalometer (Model 451, GraLab) and set to a cycle of 20 s on and 60 s off. The control plate was kept in the dark throughout the experiment. Forty-eight hours after transfection, firefly and *Renilla* luciferase activity was measured using the Dual-Glo luciferase assay kit (Promega) according to the manufacturer's instructions. The following equation was used to determine the normalized fold change in transcription in the dark and with light between cells expressing pVP-EL222 and pVP-empty: fold change = $(\text{Fluc/Rluc})_{\text{VP-EL222}}/(\text{Fluc/Rluc})_{\text{empty}}$.

For transfection of the 293T VP-EL222 stable line, cells were plated 1 d before transfection at 1×10^5 cells ml^{-1} in 24-well plates. The next day, 0.8 μg of pcDNA-C120-Fluc DNA were transfected using lipofectamine. Immediately afterward, the cells were illuminated using a LED panel (20 s on, 60 s off) for 12 h, unless otherwise indicated in the legend (**Figs. 1** and **2** and **Supplementary Figs. 1** and **2**). For experiments done with JSL1 cells, wild-type or VP-EL222/C120-Flag-CELF2 stable cells were plated at 6×10^5 cells per well in six-well plates. The next day, cells were illuminated (20 s on, 60 s off) for 24 h and subsequently harvested for western blotting and RT-PCR analysis. The viability of 293T cells was evaluated using the Cell Titer Blue assay (Promega) according to the manufacturer's instructions.

Nuclear and cytoplasmic extract isolation and western blotting. 293T cells (5.4×10^6 cells total) were grown in 10-cm dishes and were transfected with pVP-EL222 or left untreated. Forty-eight hours after transfection, nuclear and cytoplasmic extracts were purified using the following protocol. Cells were harvested and pelleted by centrifugation for 5 min at 3,220*g*. The pellet was resuspended in 1 ml of ice-cold PBS, centrifuged for 5 min at 100*g* and resuspended in 1 ml ice-cold Buffer A (10 mM Tris-Cl, pH 7.5, 1.5 mM $MgCl_2$, 10 mM KCl). The cell suspension was incubated on ice for 5 min, in a dry ice–ethanol bath for 5 min and in a 37 °C water bath for 5 min. This incubation series was repeated two more times. Afterwards, the cells were centrifuged at 4 °C for 15 min at 15,900*g*. The supernatant (nuclear extract) was moved to a new tube, and the pellet (cytoplasmic extract) was resuspended in 1 ml Buffer A.

For western blotting, equal protein amounts of total cell lysates were separated on a 10% Mini-PROTEAN TGX precast gel (BioRad) and then transferred to a polyvinylidene fluoride (PVDF) membrane (Amersham). The protein signal was detected using the Pierce ECL western blotting Substrate (Thermo Scientific) according to the manufacturer's instructions. The antibodies used were as follows: anti-VP16 AD (ab4808, Abcam; 1:2,000 dilution), anti-luciferase (L0159, Sigma; 1:1,000 dilution), anti–β-actin (A5441, Sigma; 1:20,000 dilution), anti-ARNT (sc-17811, Santa Cruz Biotechnology; 1:500), anti–hnRNP L (ab6106, Abcam; 1:1,000 dilution) and anti-Flag (2368, Cell Signaling; 1:1,000).

Pre-mRNA splicing analysis. RNA isolation and analysis of pre-mRNA splicing by RT-PCR were done as described previously for JSL1 cells[28,41]. Primers for the analysis of the endogenous CELF2 gene are as follows: forward primer in the 5′-UTR region, 5′-TCTGCTCGACAGCAGCACGCAGTG-3′; reverse primer downstream of variable exon 6, 5′-CAGGTGGCAGTGTTGAGCTGC-3′.

Quantitative PCR analysis. Total RNA was isolated from transfected wild-type 293T and VP-EL222 cells using an RNeasy kit (Qiagen) following the manufacturer's instructions. Four micrograms of total RNA were treated with DNase I (NEB) to remove genomic DNA. One microgram of each treated RNA sample was reverse transcribed using iScript cDNA synthesis kit (BioRad). qPCR was performed on a Applied Biosystems 7300 real-time PCR system using TaqMan Fast Advanced Master Mix and TaqMan Gene Expression Assays for Luciferase and GAPDH (Applied Biosystems) with 100 ng of cDNA as template. Samples were run in triplicate, and the average cycle threshold (C_T) was calculated. The average luciferase C_T value for each sample was normalized to the corresponding average GAPDH C_T value to obtain a ΔC_T value. The fold change in luciferase mRNA expression in VP-EL222 cells relative to wild-type 293T samples was calculated using the comparative C_T ($\Delta\Delta C_T$) method[42].

Live cell fluorescence microscopy. Wild type or VP-EL222 stable 293T cells were transfected with pC120-mCherry plasmid immediately after the cells were illuminated for 24 h (20 s on, 60 s off) or left in the dark. Cells were examined on a Nikon Eclipse TS100 epifluorescence microscope running NIS Elements and equipped with Photometrics Coolsnap HQ camera. Images were taken with a 10×/0.25 NA Achromat Ph1 objective, and mCherry fluorescence was imaged with a G2A filter. Image processing and analyses were performed using ImageJ software[43].

Zebrafish strains. Adult zebrafish, both TL and AB wild-type strains, were maintained under standard laboratory conditions[44]. Husbandry and experimental protocols for zebrafish studies were approved by the International Animal Care and Use Committee.

Transient expression and light induction in zebrafish. Expression plasmid pCS2-VP-EL222 was created by PCR amplification of VP-EL222 ORF and then cloned into pCS2+ (gift from S. Woo, University of California–San Francisco). Capped messenger RNA was synthesized using the mMESSAGE mMACHINE SP6 kit (Ambion). Fifty picograms of VP-EL222 mRNA and/or 20 pg of pGL4-C120-mCherry plasmid DNA were injected at the one-cell stage. For heart-specific expression of VP-EL222 and light-induced induction of mCherry reporter, VP-EL222 ORF and C120-mCherry promoter and ORF were PCR amplified and cloned into pminiTol2-*myl7* (refs. 45,46) to create the dual promoter construct, pminiTol2- *myl7*-VP-EL222-C120-mCherry. Twenty picograms of pminiTol2-*myl7*-VP-EL222-C120-mCherry plasmid DNA along with 50 pg of Tol2 transposase mRNA were injected at the one-cell stage.

Constant blue light was applied at approximately 2 h.p.f. with a blue LED panel (465 nm, 2501BU, LED Wholesalers). The actual power of light received by embryos was measured to be ~1 mW using a PM100D Laser Power and Energy Meter Console (Thorlabs). Dark controls were placed in a lightproof box in the same 29 °C incubator as light-treated samples. The light was turned off at 24 h.p.f. for imaging and analysis of embryos. For heart-specific induction of mCherry, constant light was applied from 10 h.p.f. to 24 h.p.f.

Microscopy and image processing of zebrafish embryos. Fluorescent and bright field images at 70% epiboly were taken on a Digital Scanned Laser Light Sheet Microscope[47]. Embryos were mounted in a 1.5% low-melt agarose

cylinder using 3 mm O.D.–2 mm I.D. FEP tubing (Bola). *Z*-stacks of 2.58-µm intervals were taken with a 10×–0.5 NA objective. mCherry fluorescence was imaged with 561 nm laser line and a 561LP filter. Bright field images were acquired using room light. Fluorescent and bright field images at 24 h.p.f. were taken on a Nikon Eclipse Ti microscope running NIS Elements and equipped with a Lambda XL Broad Spectrum Light Source (Sutter) and an iXon DU-897 EMCCD camera (Andor).

Dechorionated embryos were embedded in 1.5% low-melt agarose within glass-bottom Petri dishes (MatTek Corporation). Whole-embryo images were taken with a 4×–0.13 NA Plan-Fluor objective, and heart-specific images were taken with a 20×–0.75 NA Plan Apo objective. Standard filter settings were applied. Image processing and analysis was performed using ImageJ software[43]. For the 70% epiboly images, maximum intensity projections of the fluorescent *Z*-stack were performed and merged with a corresponding bright field image. For whole-embryo and heart-specific 24-h.p.f. images, mCherry and bright field channels were merged.

Toxicity curves in zebrafish. At the one- to two-cell stage, 50 pg, 100 pg, 150 pg, 200 pg or 300 pg of VP-EL222 or GFP (control) mRNA per embryo were injected. Unfertilized embryos were removed on day 0, and phenotypes of each group were scored alongside uninjected control embryos from the same clutch on day 1 after manual dechorionation. The experiment was performed under constant blue light conditions (465 nm). Each group had at least $n = 100$ embryos. Embryos were scored as follows: normal to unaffected embryos were considered to have a wild-type phenotype; embryos with the presence of a slightly curved tail and/or mild edema were considered mildly deformed; embryos with smaller heads, major curves or a kink in the tail and/or severe edema were considered severely deformed.

Statistics. Data are represented as mean values ± s.d. For statistical analysis, a two-tailed Student's *t*-test was applied to test rejection of the null hypothesis. *P* values less than 0.05 were considered statistically significant.

41. Lynch, K.W. & Weiss, A.A. CD45 polymorphism associated with multiple sclerosis disrupts an exonic splicing silencer. *J. Biol. Chem.* **276**, 24341–24347 (2001).
42. Bookout, A.L. & Mangelsdorf, D.J. Quantitative real-time PCR protocol for analysis of nuclear receptor signaling pathways. *Nucl. Recept. Signal.* **1**, e012 (2003).
43. Schneider, C.A., Rasband, W.S. & Eliceiri, K.W. NIH Image to ImageJ: 25 years of image analysis. *Nat. Methods* **9**, 671–675 (2012).
44. Westerfield, M. *The Zebrafish Book. A Guide for the Laboratory Use of Zebrafish (Danio rerio)* 5th edn. (The University of Oregon Press, 2007).
45. Balciunas, D. *et al.* Harnessing a high cargo-capacity transposon for genetic applications in vertebrates. *PLoS Genet.* **2**, e169 (2006).
46. Huang, C.J., Tu, C.T., Hsiao, C.D., Hsieh, F.J. & Tsai, H.J. Germ-line transmission of a myocardium-specific GFP transgene reveals critical regulatory elements in the cardiac myosin light chain 2 promoter of zebrafish. *Dev. Dyn.* **228**, 30–40 (2003).
47. Maizel, A., von Wangenheim, D., Federici, F., Haseloff, J. & Stelzer, E.H. High-resolution live imaging of plant growth in near physiological bright conditions using light sheet fluorescence microscopy. *Plant J.* **68**, 377–385 (2011).

doi:10.1038/nchembio.1430